Materials Science and Engineering C 74 (2017) 117–123

Contents lists available at ScienceDirect

Materials Science and Engineering C

journal homepage: www.elsevier.com/locate/msec

Melt electrospinning vs. solution electrospinning: A comparative study of drug-loaded poly (ε-caprolactone) fibres

He Lian, Zhaoxu Meng *

Department of Biomedical Engineering, School of Medical Devices, Shenyang Pharmaceutical University, No. 103, Wenhua Road, Shenyang 110016, China

ARTICLE INFO

Article history:
Received 4 September 2016
Received in revised form 10 December 2016
Accepted 6 February 2017
Available online 7 February 2017

Keywords:
Melt electrospinning
Solution electrospinning
Drug release
Polycaprolactone
Curcumin

ABSTRACT

Curcumin-loaded poly (ε-caprolactone) (PCL) fibres prepared by melt and solution electrospinning methods were both fabricated to investigate their difference in characterization and drug release behaviour. The increasing curcumin content did not influence the morphologies of melt electrospun fibre, but enhanced the range of diameter distribution of solution electrospun fibre owing to the curcumin aggregates in the spinning solution which disturbed the stability of jet. Moreover, a large amount of curcumin with amorphous state could be loaded in the melt electrospun fibre. Whereas the limited solubility of curcumin in the solvent led to the drug aggregates dispersing within the solution electrospun fibre. In addition, the melt electrospun fibres had low drug release rate without burst release on the profiles due to the high crystallinity in the fibre, but high drug release rate and burst release occurred on the release profiles of the solution electrospun fibres because of their low crystallinity, porous structure and roughness surface.

1. Introduction

Among the various materials developed for drug-carrier applications, electrospun fibres from natural and synthetic polymers have been reported [1–6]. Drug delivery systems (DDS) based on electrospun fibrous membranes have been extensively studied because they exhibit high surface-to-volume ratio, important porosity, and controllable morphology [7–12]. In addition, drug-loading methods for electrospun materials, such as direct mixing or core-shell loading, are in continuous development as noticed by the increasing number of publications in this field [13–16]. It is to be noted that most of the studies refer to solution rather than melt electrospinning techniques. These two techniques differentiate themselves by several characteristic properties. Indeed, solution electrospinning requires a compatible solvent able to dissolve a given polymer and the drug to form a homogenous solution, which is then submitted to a high voltage that forms an ultrafine jet that is ejected from the charged solution and then transformed into fibres by solvent evaporation [17–19]. In contrast, melt electrospinning is a solvent-free method in which the fibre is formed by cooling the melt jet ejected from the charged polymer melt composed of the polymer matrix and the drug [20,21]. Moreover, various types of materials and drugs can be processed by solution electrospinning without specific restrictions. However, most of biological molecules such as protein, polysaccharide, and nucleic acid, and thermosensitive polymers cannot be treated by melt electrospinning [22–24]. Finally, solution electrospinning requires an appropriate solubility of low molecular drugs in the spinning solution [25–29]. In consequence, the drug loading capacity largely depends on the selection of the solvent, which remains a challenge because both the polymer and the drug are to dissolve inside the spinning solution. Actually, the drug content is usually reduced in the benefit of obtaining a higher polymer concentration than the threshold viscosity [30]. In contrast, melt electrospinning involves the direct mixing of the drug in the polymer melt.

Despite the many disadvantages, solution electrospinning remains the most studied and applied technique for loading drugs in electrospun fibres because of the simple equipments and no restrictions of polymers and drugs. However, melt electrospinning is a safer and "greener" method than solution electrospinning as it presents the advantages of no solvent residual or release, excellent biomedical safety, a large amount of drug loading among others. So far, melt electrospinning applied for DDS is at its infancy phase as supported by the low number of published studies in this field. Nagy et al. demonstrated that melt electrospinning permitted to enhance the loading of a water-poor soluble molecule resulting in a fast drug release [25,26]. Consequently, many opportunities are open for the development of DDS based on melt electrospinning and a better knowledge of this technique is required. As examples, the drug release behaviours of melt electrospun fibres fabricated from hydrophobic polymers or the efficiency of drug release between melt and solution electrospun fibres are issues among others to be studied.

Therefore, this study contributes to this new field by comparing the characteristics between melt and solution electrospun fibres. Although

* Corresponding author.
E-mail address: mengzhaoxu2006@163.com (Z. Meng).

http://dx.doi.org/10.1016/j.msec.2017.02.024
0928-4931/

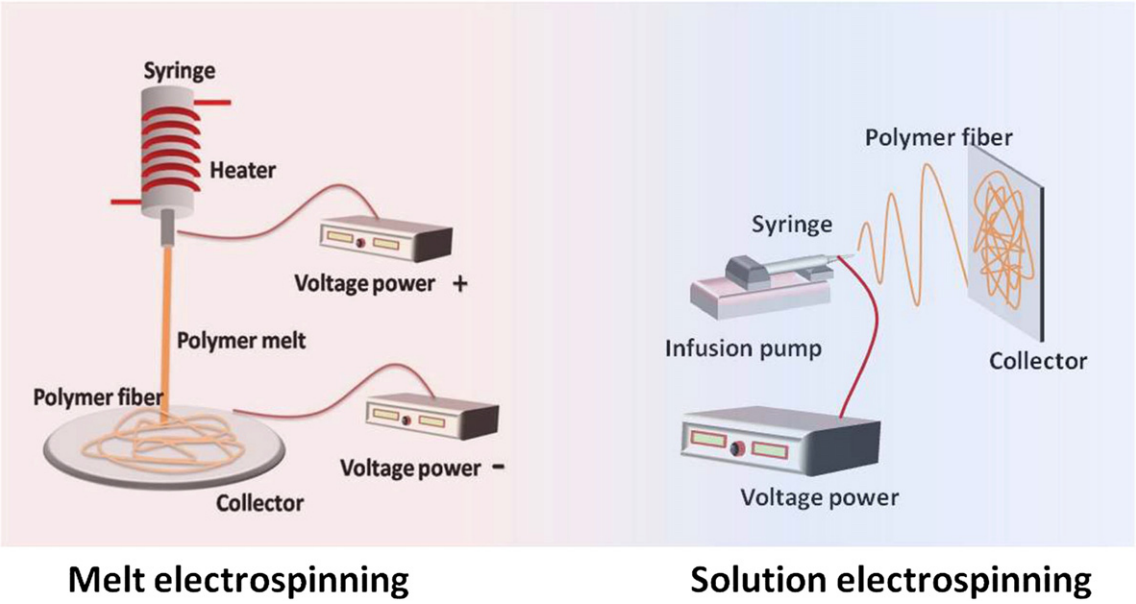

Scheme 1. Apparatus of melt electrospinning and solution electrospinning.

several polymers were already investigated in melt electrospinning, biodegradable polymers have surprisingly attracted least attention. Indeed, biodegradable polymers present the advantage to be able to degrade into small molecules that could be naturally discarded from the Human body [31–33]. Poly (ε-caprolactone) (PCL) is an approved FDA aliphatic polyester that has attracted increasing interest in many fields due to its excellent biocompatibility [34–36]. Moreover, according to previous reports, PCL has one of the lowest melting points among the hydrophobic polymers and decomposes at high temperature [37–39]. These features are suitable for melt encapsulating many drugs in a wide temperature range. We have selected curcumin as it is an anticancer drug with excellent fluorescence property, allowing the easy observation of its dispersion inside the matrix. Furthermore, curcumin exhibits a suitable thermal stability allowing the drug activity not to be affected during the melt electrospinning [40]. This study describes the use of PCL as drug delivery carrier and curcumin as the model drug. The physic-chemical properties of the drug-loaded PCL fibres fabricated by melt and solution electrospinning were compared.

2. Materials and methods

2.1. Materials

Poly (ε-caprolactone) (M_w = 40.000) was purchased from Shenzhen Polymtek Bomaterial Co. Ltd. (China). Curcumin (CAS: 458-37-7) was purchased from Dalian Meilun Biology Technology Co. Ltd. (China). Dichloromethane and ethanol (analytical reagent grade) were purchased from Tianjin Chemical Reagent Company (China) as the

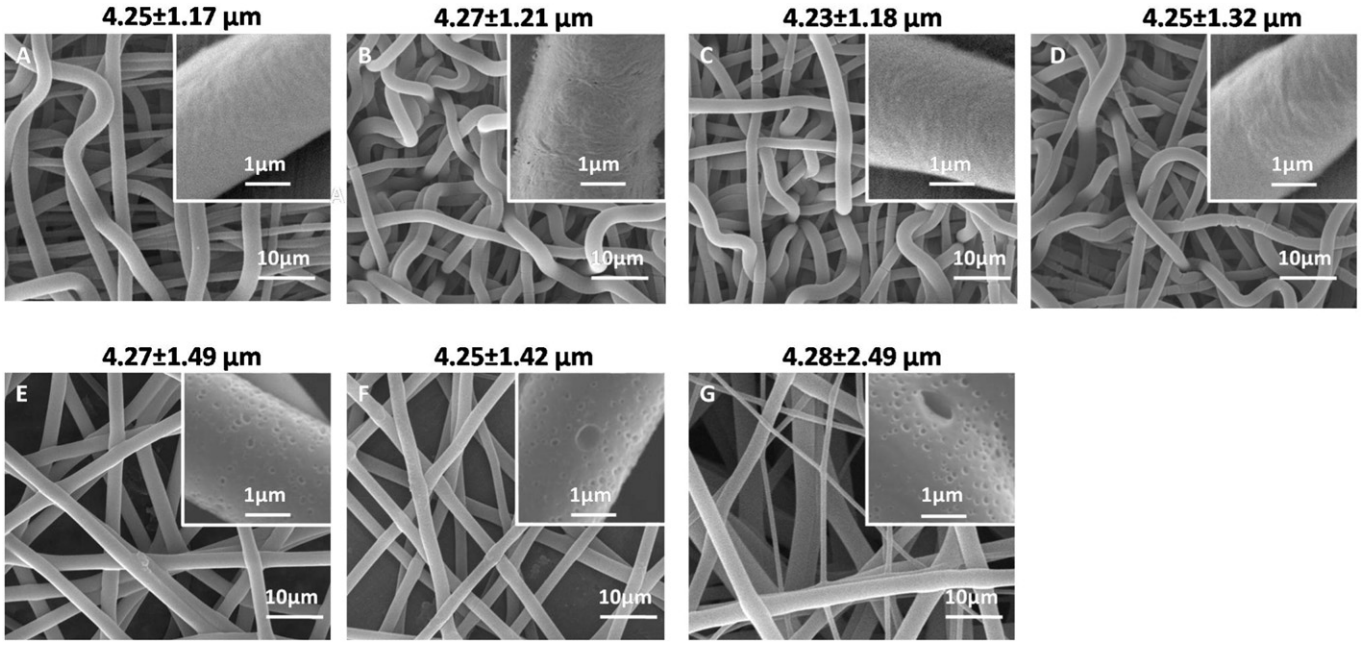

Fig. 1. SEM images of PCL melt electrospun fibres (A), curcumin-loaded PCL melt electrospun fibres (B: 1 wt%, C: 5 wt%, D: 10 wt%), PCL solution electrospun fibres (E) and curcumin-loaded PCL solution electrospun fibres (F: 1 wt%, G: 5 wt%).

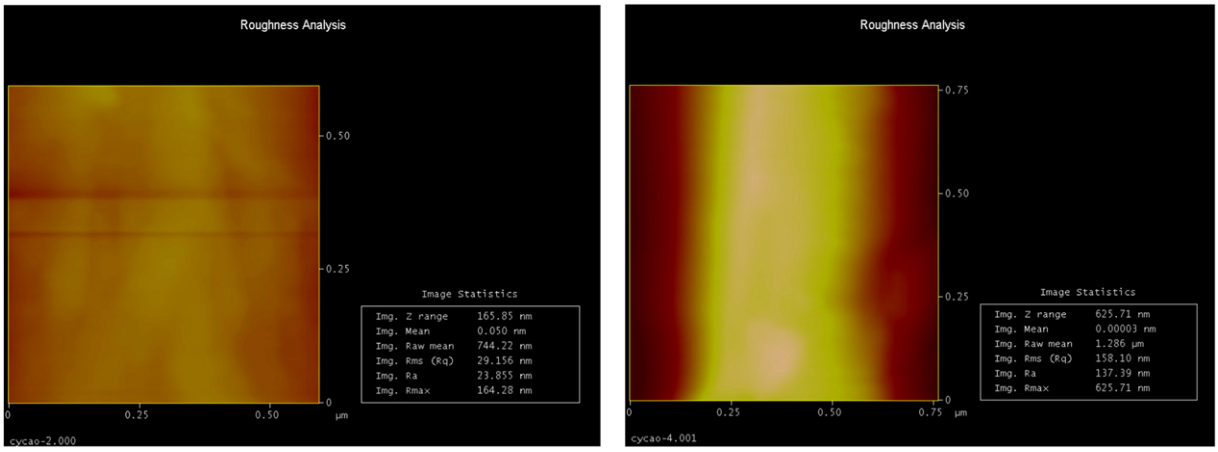

Fig. 2. AFM topography images and analysis of the surface roughness of PCL ME and SE fibres.

solvent in the solution electrospinning. All the chemicals were used directly without further purification and aqueous solutions were prepared with doubly distilled water.

2.2. Fabrication of drug-loaded melt and solution electrospun fibres

The preparation of drug-loaded PCL melt electrospun fibres was demonstrated as follows: PCL was heated into melt at the temperature of 180 °C and curcumin (1 wt%, 5 wt% and 10 wt% to PCL) was added into the PCL melt and stirred for 1 h to ensure a homogeneous fluid. And then, the fluid was transferred to melt electrospinning apparatus which was shown in Scheme 1. During the melt electrospinning, the heater was kept at the temperature of 180 °C, and a high voltage of +20 kV was applied to the melt and voltage of −10 kV was connected to the flat collector keeping at a distance of 15 cm from the needle.

The drug-loaded PCL fibres from solution electrospinning were fabricated as following: PCL was dissolved in the dichloromethane/ethanol (v:v = 3:1) composite solvent with the concentration of 20 wt%, and then curcumin was added into the solution (1 wt% and 5 wt% to PCL). The solution was stirring for 12 h and then electrospun into fibre with the apparatus in Scheme 1. The syringe filled with composite solution was placed on the infusion pump with an injection rate of 0.5 mL/h, and the stainless steel blunt needle fitted on the syringe was applied with a high voltage of +10 kV. The drug-loaded PCL fibres were collected on the metal plant which was 10 cm far from the needle tip. The obtained fibres were dried in vacuum dying oven overnight at room temperature.

2.3. Characterization

The morphologies of the fibres were characterized by scanning electron microscopy (SEM) (FE-SEM Model JSM-7011F, Japan) at an accelerating voltage of 15 kV, and all the samples were drying under vacuum for 24 h and then coated with a thin layer of gold to produce

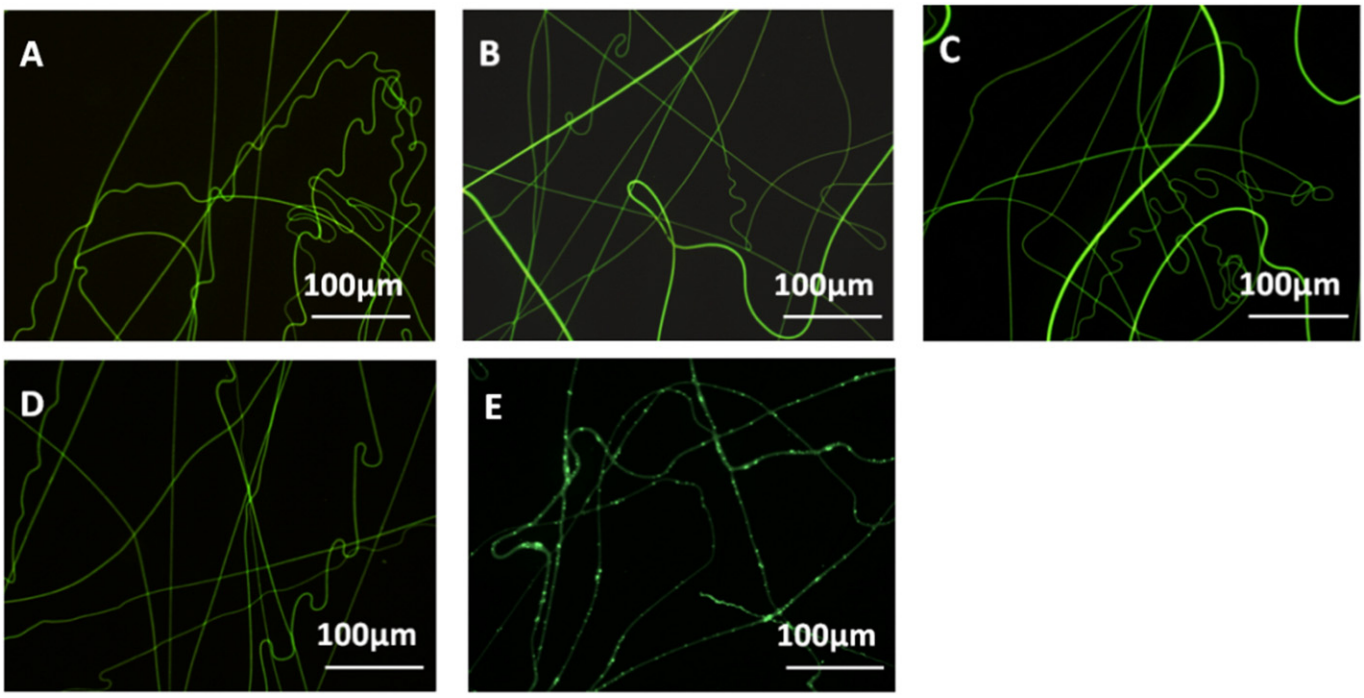

Fig. 3. Fluorescence images of curcumin-loaded PCL melt electrospun fibres (A: 1 wt%, B: 5 wt% and C: 10 wt%) and solution electrospun fibres (D: 1 wt% and E: 5 wt%).

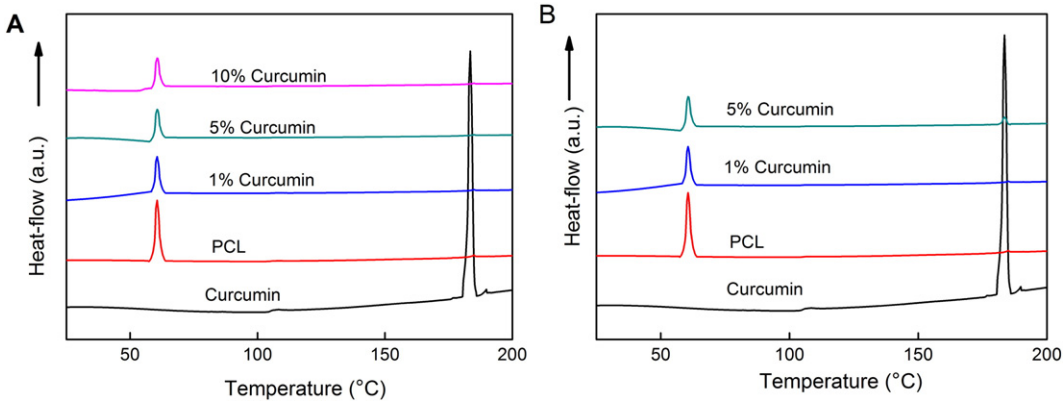

Fig. 4. DSC thermograms of curcumin powder, curcumin-loaded PCL melt electrospun fibre (A), and solution electrospun fibre (B).

a conductive surface. The diameters of resulting fibres were analysed using software Image J. A fluorescence microscopy (Olympus BX53, Japan) was used to observe the fluorescence from the drug-loaded fibres. A differential scanning calorimeter (DSC) (Perkin–Elmer Company, USA) was adopted to investigate the thermal property of all the samples with a temperature range from −50 °C to 300 °C at a heating rate of 15 °C /min under a nitrogen atmosphere. FT-IR spectra were recorded for drug-loaded fibrous mashes in the ATR mode using an IR spectrophotometer (Nicolet iS5, USA) and the spectra were ranging from 4000 to 400 cm^{-1} with a resolution of 4.0 cm^{-1} and 16 scans. X-ray diffraction analysis was characterized by X-ray diffractometer (Bruker D8 Advance, Germany) equipped with Cu-Kα source and operating at 40 kV and 100 mA. The diffraction patterns were obtained at a scan rate of 1°/min. The roughness of the fibre was evaluated by Atomic Force Microscopy (Bruker Multimode 8, Germany).

2.4. Drug release

The samples were dissolved in 5 mL dichloromethane/ethanol (v:v = 3:1) composite solution and measured by a UV–Vis spectrometer (Shimadzu UV-2550, Japan) at the wavelength of 425 nm. The actual drug amount in the sample was back calculated from the obtained data against a predetermined calibration curve of curcumin ($y = 0.2640x - 0.0199$, $R^2 = 0.9996$, where y is the concentration of curcumin). The calibration curve of FBF was carried out in the concentration ranging from 0.001 mg/mL to 0.01 mg/mL.

The drug-loaded sample was incubated in 1000 mL of PBS (pH = 7.4) at 37 °C. At various time points, 2 mL of the release medium was taken out and replaced by fresh PBS. The amount of released drug was determined using the UV–vis spectrophotometer at the wavelength of 425 nm.

2.5. Statistical analysis

A software of origin 8.0 (Origin Lab Inc., USA) was used to analyze the obtained data. Values (n = 3) were averaged and expressed as means ± standard deviation (SD).

3. Results and discussion

3.1. Morphologies

In order to avoid misinterpretation of experimental data that could be due to the difference in the diameter of the studied fibres, we isolated fibres exhibiting similar diameters from the production of melt electrospinning (ME) and solution electrospinning (SE). More specifically, the isolated ME and SE fibres had diameters of 4.25 ± 1.17 and 4.27 ± 1.49 μm, respectively. Curcumin-loaded PCL fibre were prepared via melt and solution electrospinning and characterized by following experiments.

The morphology of the electrospun fibre significantly depended on the fabrication method. As shown by the SEM images of Fig. 1, we could observe fine wrinkles on the surface of the ME fibres (Fig. 1A–

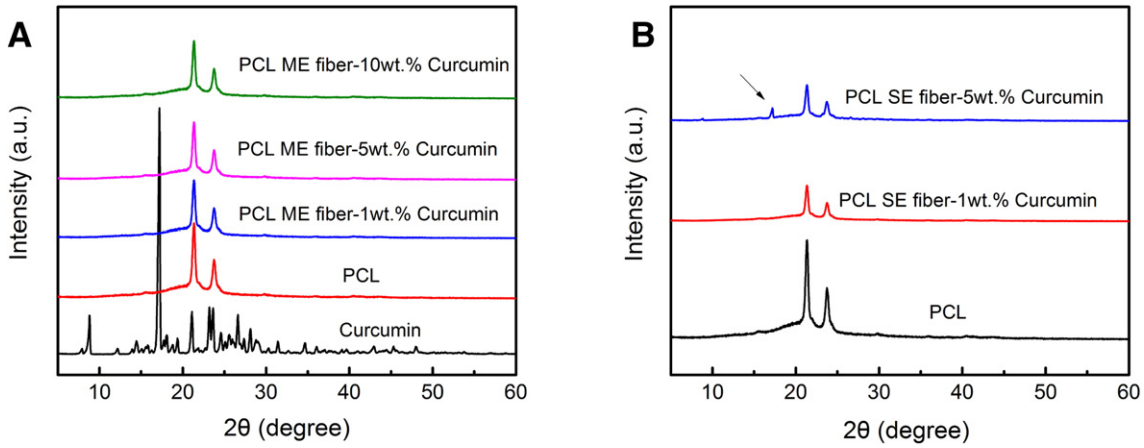

Fig. 5. XRD patterns of curcumin powder, PCL, curcumin-loaded PCL melt electrospun fibre (A), and solution electrospun fibre (B).

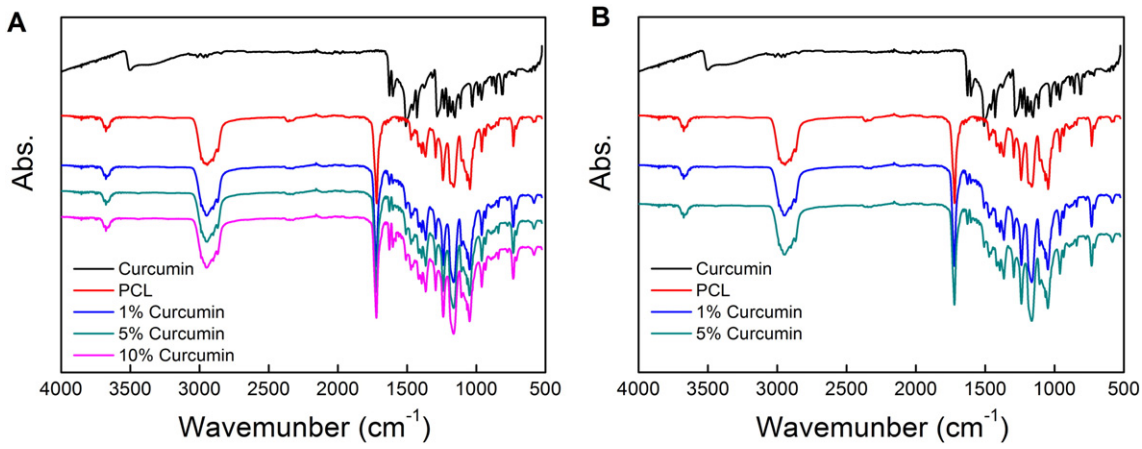

Fig. 6. FT-IR spectra of curcumin powder, curcumin-loaded PCL melt (A) and solution electrospun fibres (B).

D), which were caused by melt contraction during the condensation process [41]. In contrast, the surface of the SE fibre presented many holes having diameters of tens to hundreds nanometers (Fig. 1E–G). Indeed, solution electrospinning involved the use a hybrid solvation system in order to fully dissolve the polymer and the drug. The difference in the boiling point of the solvents produced phase separation in the jet, resulting in the formation of small pores on the surface of the fibre [42,43].

Moreover, all the curcumin-loaded ME fibres, even the ones containing up to 10 wt% of drug, resulted in similar morphologies compared to the unloaded PCL ME fibre. In addition, there was no significant difference of the fibre diameters when preparing the fibres with different amounts of drug, indicating that the addition of the drug did not affect the morphology of the ME fibres (Fig. 1H). However, due to the limited solubility of curcumin in ethanol, the clear mixture solution containing 1 wt% of drug gradually became turbid when the drug content increased until the appearance of solid deposit when the amount of drug was more than 5 wt%. Therefore, we selected to study SE fibres containing 1 wt% and 5 wt% of drug. The micrographs depicted in Fig. 1F and G indicated that the addition of drug did not alter the fibre surface but increased the diameter distribution of the fibres. These observations demonstrated that the drug aggregates increased the instability of the jet during solution electrospinning.

The surface of the fibres were further analysed by atomic force microscopy (AFM) to determine the surface roughness of the PCL ME and SE fibres. The topography images illustrated in Fig. 2 show that the SE fibres (average roughness 158.10 nm) exhibited a higher roughness than ME fibres (average roughness 29.16 nm). The results, consistent with the previous SEM images, could be attributed to the difference in fabrication involved in melt and solution electrospinning processes [41].

3.2. Fluorescence

Since the drug was directly introduced into the drug carrier in the case of melt electrospinning, the dispersion of the drug was an important factor as the different aggregate states of the drug in the polymer might have an impact on the release profile of the drug [44]. In this study, we intentionally selected curcumin as it has a convenient fluorescence property that made the observation of the drug dispersion in the fibre easy. The fluorescent images of curcumin-loaded PCL ME and SE fibres are shown in Fig. 3. The pictures clearly revealed the incorporation of the drug in the ME fibres loaded with curcumin in the range of 1 wt% to 10 wt% (Fig. 3A–C), suggesting that curcumin and PCL were homogeneously mixed under the molten state. The successful result could be explained by the fact that curcumin and the polymer are both hydrophobic, which facilitated the compatibility of the drug in PCL. However, many green bright spots of curcumin aggregates could be observed among the SE fibres when the drug amount reached 5 wt% (Fig. 2E), indicating that curcumin was not completely dissolved in the spinning solution.

3.3. Thermal properties

To further validate the drug incorporation inside the ME and SE fibres, the samples were analysed by differential scanning calorimetry (DSC) to characterize the thermal properties of curcumin powder, pure and curcumin-loaded PCL ME and SE fibres. The results are shown in Fig. 4. The endothermic curve of curcumin powder exhibited an important peak at about 184 °C corresponding to the melting point of the curcumin [40]. The peak observed at 61 °C on the PCL thermogram arose from the melting transition of the unloaded polymer [38,39]. As shown in the results presented in Fig. 4A, no significant peak was observed on the curves of PCL ME fibres loaded with curcumin at 1 wt% and 5 wt% except for the a very discrete peak characteristic of the melting temperature of curcumin when the drug content was 10 wt%. In contrast, a significant peak occurred on the thermogram of SE fibre containing 5 wt% curcumin as illustrated in Fig. 4B (details was seen in SI). According to other reported studies, this peak could be attributed to the fact that the drug could be distributed in the ME fibre under the amorphous and crystalline states in the SE fibre [40,45].

3.4. XRD analysis

The prepared samples (PCL ME and SE fibres) were further subjected to XRD and the results are shown in Fig. 5. The XRD patterns indicated that no diffraction peaks of curcumin appeared on the curves of the ME fibres, suggesting that the drug was under an amorphous state [46]. In contrast, the characteristic peak of crystalline curcumin was observed for the SE fibres ($2\theta = 17.5°$Fig. 5B), indicating that the drug was under a crystal state [47]. In addition, the degree of crystallinity of the ME fibres was higher than the one of the SE fibres according to the

Table 1
Actual amount of curcumin in curcumin-loaded PCL melt and solution electrospun fibres.

Samples	Actual amount of curcumin based on the initial amount of curcumin loaded (%)	
	Melt electrospinning fibre	Solution electrospinning fibre
PCL-1 wt% curcumin	98.68 ± 1.45	98.89 ± 1.02
PCL-5 wt% curcumin	99.03 ± 1.98	93.14 ± 6.47
PCL-10 wt% curcumin	98.76 ± 1.55	–

intensity of the diffraction peaks of the XRD patterns. These observations indicated that the formation of PCL crystals was favoured under the melt conditions. Previous studies reported that several approaches could improve the crystallinity of the fibre when prepared via solution electrospinning, such as increasing the stability of the jet or decreasing the solution concentration [48,49]. However, the melt jet travels in a straight path without the whipping instabilities and no solvent was used in the in melt electrospinning, so the crystallinity of ME fibre was higher than SE fibre [41].

3.5. FT-IR spectroscopy

The FT-IR spectra of the samples are presented in Fig. 6. The spectrum of curcumin powder exhibited a characteristic absorption band of phenolic O—H stretching vibrations at 3503 cm^{-1}, the band at 1627 cm^{-1} was attributed to the carbonyl stretching vibrations of the conjugated ketone, and the one appearing at 1602 cm^{-1} was due to the benzene ring stretching vibrations. Moreover, the bands at 1504 and 1429 cm^{-1} were attributed to the stretching vibrations of the C—C bonds of the benzene ring and to the olefinic bending vibrations of the C ═C bonds bound to the benzene ring, respectively [50,51]. The main peaks of 1627 and 1602 cm^{-1} were also clearly observed in the spectrum of ME fibre (Fig. S2). The intensity of the signals became more intensive as the curcumin content increased. The changes in the other characteristic signals of curcumin were difficult to evaluate in the fibres spectra due to the overlapping of the PCL vibration bands. Similarly, the main peaks of curcumin appearing at 1627 and 1602 cm^{-1} were also present in the FT-IR spectrum of the SE fibres (Fig. 6B). Interestingly, the position of the characteristic curcumin peaks did not move in the fibres" spectra, suggesting the absence of intermolecular interactions between curcumin and PCL [52].

3.6. Drug release

Studies published in the literature reported that the curcumin decomposes in the approximate range of 237 to 248 °C [40,52,53]. As the melt temperature of PCL is lower than the decomposition temperature of curcumin, we selected curcumin as a model drug to investigate the release behaviour from the ME and SE fibres. Moreover, the antitumor effect of curcumin was verified prior to the drug release experiment consisting of a heat treatment (Fig. S3) [46]. The results indicated that heat treatment did not influence the bioactivity of curcumin.

The actual amounts of curcumin in the PCL ME and SE fibres were calculated and listed in Table 1. The actual curcumin contents in the PCL ME fibre were all higher than 98% and remained at the same value even if the added portion of the drug increased in the preparation. However, the value of the SE fibre prepared with 5 wt% of curcumin was slightly lower than the one ME fibre, which was due to the inhomogeneous dispersion of the drug inside the fibre.

Two distinct differences could be observed from the in vitro release profiles of curcumin from PCL ME and SE fibres (Fig. 7). First, the release rates of the ME fibres were much lower than that of the SE fibres. After two weeks, the values of the release ratio were 3.35%, 12.72%, and 23.99%, corresponding to the ME fibres with drug contents of 1 wt%, 5 wt%, and 10 wt%, respectively. Comparatively, the release ratios of the SE fibres exhibited higher values with drug contents of 1 wt% and 5 wt% were 33.05% and 56.48%, respectively. In addition, the release profiles of the SE fibres presented a higher burst release compared with the ones of the ME fibres. No burst release behaviour was observed in the curves of ME fibres containing 1 wt% and 5 wt% curcumin. Only the curve of the ME fibre containing 10 wt% of curcumin revealed a slight trend for a burst release at the initial stage.

The observations could be explained as follows. Firstly, the morphological differences of the ME and SE fibres led to different drug releases mechanisms. Curcumin molecules could be released from the SE fibres via the characteristic porous structure and rough surface, which offered an enhanced contact area with the surrounding medium and also promoted medium penetration [54]. In addition, the shortened diffusion distances inside the SE fibres supported the drug release. Secondly, the higher degree of crystallinity of the ME fibres compared to the one of the SE fibres, which was observed by XRD (Fig. 5), was another important factor affecting the drug release. The ordered molecular chains of a crystal region of a polymer could inhibit the diffusion of the medium into the region, whereas in an amorphous region of the polymer, the loosely arranged molecular chains would increase the chance of medium penetration [55,56]. Thirdly, the SEM images (Fig. S4) showed that the fibres overlapped during the release process due to fusion. This behaviour could be due to the molecular chain of the amorphous region of the fibres that could diffuse into the adjacent region by heat motion [57]. Since the amorphous regions in the SE fibres were more important than in the ME fibres, fusion in the SE fibres were more obvious. In parallel, the motion of the molecular chains also promoted drug diffusion out of the fibres. Therefore, the differences in the preparations of melt and solution electrospinning techniques led to distinguished morphologies and internal structures, which resulted in a lower drug release rate from the ME fibres than that from the SE fibres.

4. Conclusions

In summary, we fabricated curcumin-loaded PCL ME and SE fibres, and investigated their difference in characteristics and drug release behaviours. The PCL melt electrospun fibres presented a smooth surface

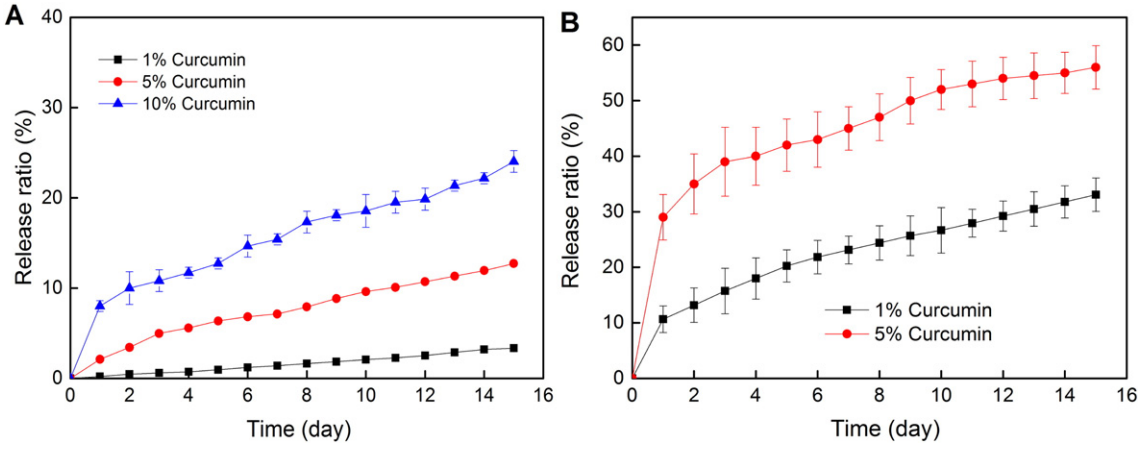

Fig. 7. In vitro release curves of curcumin from PCL melt (A) and solution electrospun fibres (B).

and high crystallinity, whereas the PCL solution electrospun fibres exhibited a porous structure and more amorphous regions than the PCL ME fibres. A large amount of drug, under an amorphous state, was distributed inside the ME fibres. In contrast, drug aggregates were encapsulated inside the SE fibres due to the limited drug solubility in the solvent. Moreover, the melt electrospun fibres could release the drug slowly without a burst phase, thanks to the high crystalline character of the fibres. In opposite, a high drug release rate with a burst release behaviour was observed in the solution electrospun fibres because of their low crystallinity, porous structure, and rough surface. Therefore, the PCL melt electrospun fibres were more suitable than PCL solution electrospun fibres for a DDS application as the previous ones showed as low release rate of the drug during a long period.

Acknowledgements

This work is supported by the Scientific Research General Project of Liaoning Provincial Department of Education (No. L2014388), the Natural Science Foundation of Liaoning Province (No. 2015020753), and National Natural Science Foundation of China (No. 81503020, No. 31600764).

Appendix A. Supplementary data

Supplementary data to this article can be found online at http://dx.doi.org/10.1016/j.msec.2017.02.024.

References

[1] A. Seham, Khaled M. Honsy, K. Mallesh, J. Eng. Fiber. Fabr. 10 (2015) 179–193.
[2] G. Panthi, M. Park, H.Y. Kim, S.J. Park, J. Ind. Eng. Chem. 24 (2015) 1–13.
[3] M. Mehrasa, M.A. Asadollahi, B. Nasri-Nasrabadi, K. Ghaedi, H. Salehi, A. Dolatshahi-Pirouz, A. Arpanaei, Mater. Sci. Eng. C 66 (2016) 25–32.
[4] J.M. Lee, T. Chae, F.A. Sheikh, H.W. Ju, B.M. Moon, H.J. Park, Y.R. Park, C.H. Park, Mater. Sci. Eng. C 68 (2016) 758–767.
[5] D. Li, W. Chen, B. Sun, H. Li, T. Wu, Q. Ke, C. Huang, H. El-Hamshary, S.S. Al-Deyab, X. Mo, Colloid. Surface. B 146 (2016) 632–641.
[6] R. Zhang, T. Shang, G. Yang, X. Jia, Q. Cai, X. Yang, Colloid Surface. B 144 (2016) 238–249.
[7] M. Soheila, D. Yu, D.I. Jeffery, J. Polym. Sci. Polym. Phys. 53 (2015) 1171–1212.
[8] G. Tarun, R. Goutam, Amit K. Goyal, J. Drug Target. 23 (2015) 202–221.
[9] H.Y. Mi, X. Jing, L.S. Turng, J. Cell. Plast. 51 (2015) 165–196.
[10] G. Bruni, L. Maggi, L. Tammaro, R.D. Lorenzo, V. Friuli, S. D'Aniello, M. Maietta, V. Berbenni, C. Milanese, A. Girella, A. Marini, Int. J. Pharm. 511 (2016) 190–197.
[11] N.G. Panah, P. Alizadeh, B.E. Yekta, N. Motakef-Kazemi, Ceram. Int. 42 (2016) 10935–10942.
[12] A. Calafi, N. Bormann, D. Scharnweber, B. Rentsch, B. Wildemann, Mater. Lett. 119 (2014) 119–122.
[13] M. He, H. Jiang, R. Wang, Y. Xie, C. Zhao, J. Colloid Interface Sci. 490 (2017) 270–278.
[14] C.M. Srivastava, R. Purwar, Mater. Sci. Eng. C 68 (2016) 276–290.
[15] C. Akduman, I. Özgüney, E.P.A. Kumbasar, Mater. Sci. Eng. C 64 (2016) 383–390.
[16] Z. Sultanova, G. Kaleli, G. Kabay, M. Mutlu, Int. J. Pharm. 505 (2016) 133–138.
[17] T. Jiang, E.J. Carbone, K.W.H. Lo, C.T. Laurencin, Prog. Polym. Sci. 46 (2015) 1–24.
[18] M.L. Muerza-Cascante, D. Haylock, D.W. Hutmacher, P.D. Dalton, Tissue Eng. Part B-Rev. 21 (2015) 187–202.
[19] W. Chen, D. Li, A. El-Shanshory, M. El-Newehy, H.A. El-Hamshary, S.S. Al-Deyab, C. He, X. Mo, Colloid. Surface. B 126 (2015) 561–568.
[20] N. Detta, T.D. Brown, F.K. Edin, K. Albrecht, F. Chiellini, E. Chiellini, P.D. Dalton, D.W. Hutmacher, Polym. Int. 59 (2010) 1558–1562.
[21] X. Li, H. Liu, J. Wang, C. Li, Polymer 53 (2012) 248–253.
[22] P.D. Dalton, T.D. Brown, D.W. Hutmacher, J. Tissue Eng, Regen. M. 6 (2012) 372–373.
[23] O. Mazalevska, M.H. Struszczyk, I. Krucinska, J. Appl. Polym. Sci. 129 (2013) 779–792.
[24] H. Patil, R.V. Tiwari, M.A. Repka, AAPS PharmSciTech 17 (2016) 20–42.
[25] Z.K. Nagy, A. Balogh, G. Drávavölgyi, J. Ferguson, H. Pataki, B. Vajna, G. Marosi, J. Pharm. Sci. 102 (2013) 508–517.
[26] A. Balogh, G. Drávavölgyi, K. Faragó, A. Farkas, T. Vigh, P.L. Sóti, I. Wagner, J. Madarász, H. Pataki, G. Marosi, Z.K. Nagy, J. Pharm. Sci. 103 (2014) 1278–1287.
[27] L. Weng, J. Xie, Curr. Pharm. Design 21 (2015) 1944–1959.
[28] G. Chen, Y. Lv, Curr. Pharm. Design 21 (2015) 1967–1978.
[29] K. Ulubayram, S. Calamak, R. Shahbazi, I. Eroglu, Curr. Pharm. Design 21 (2015) 1930–1943.
[30] A. Khalf, S.V. Madihally, Eur. J. Pharm. Biopharm. 112 (2017) 1–17.
[31] B.L. Farrugia, T.D. Brown, Z. Upton, D.W. Hutmacher, P.D. Dalton, T.R. Dargaville, Biofabrication 5 (2013) 25001–25011.
[32] A. Karchin, F.I. Simonovsky, B.D. Ratner, J.E. Sanders, Acta Biomater. 7 (2011) 3277–3284.
[33] C.C. Qin, X.P. Duan, L. Wang, L.H. Zhang, M. Yu, R.H. Dong, X. Yan, H.W. He, Y.Z. Long, Nanoscale 7 (2015) 16611–16615.
[34] S. Surucu, H.T. Sasmazel, Int. J. Biol. Macromol. 92 (2016) 321–328.
[35] A. Repanas, B. Glasmacher, J. Drug Deliv. Sci. Tec. 29 (2015) 132–142.
[36] K.A.G. Katsogiannis, G.T. Vladisavljević, S. Georgiadou, Eur. Polym. J. 69 (2015) 284–295.
[37] S.R. Jameela, N. Suma, A. Jayakrishnan, J. Biomater. Sci. Polym. Edn. 8 (1997) 457–466.
[38] V.K. Khatiwala, N. Shekhar, S. Aggarwal, U.K. Mandal, J. Polym. Environ. 16 (2008) 61–67.
[39] O. Persenaire, M. Alexandre, P. Degee, P. Dubois, Biomacromolecules 2 (2001) 288–294.
[40] Y. Jafari, H. Sabahi, M. Rahaie, Food Chem. 211 (2016) 700–706.
[41] T.D. Brown, P.D. Dalton, D.W. Hutmacher, Prog. Polym. Sci. 56 (2016) 116–166.
[42] K.A.G. Katsogiannis, G.T. Vladisavljević, S. Georgiadou, Eur. Polym. J. 69 (2015) 284–295.
[43] Z. Qi, H. Yu, Y. Chen, M. Zhu, Mater. Lett. 63 (2009) 415–418.
[44] I. Sebe, P. Szabó, B. Kállai-Szabó, R. Zelkó, Int. J. Pharm. 494 (2015) 516–530.
[45] K. Kadota, D. Okamoto, H. Sato, S. Onoue, S. Otsu, Y. Tozuka, Food Chem. 213 (2016) 668–674.
[46] C. Wang, C. Ma, Z. Wu, H. Liang, P. Yan, J. Song, N. Ma, Q. Zhao, Nanoscale Res. Lett. 10 (2015) 439–449.
[47] Y. Chen, J. Lin, Y. Wan, Y. Fei, H. Wang, W. Gao, Fiber Polym. 13 (2012) 1254–1258.
[48] Q.H. Zhou, M. Bao, H.H. Yuan, S.F. Zhao, W. Dong, Y.Z. Zhang, Polymer 54 (2013) 6867–6876.
[49] O. Ero-Phillips, M. Jenkins, A. Stamboulis, Polymer 4 (2012) 1331–1348.
[50] M.A. Akl, A. Kartal-Hodzic, T. Oksanen, H.R. Ismael, M.M. Afouna, M. Yliperttula, A.M. Samy, T. Viitala, J. Drug Deliv. Sci. Tec. 32 (2016) 10–20.
[51] M.H. Nguyen, H. Yu, T.Y. Kiew, K. Hadinoto, Eur. J. Pharm. Biopharm. 96 (2015) 1–10.
[52] M. Ranjbar-Mohammadi, S.H. Bahrami, Int. J. Clin. Exp. Med. 84 (2016) 448–456.
[53] S. Raj, D.R. Shankaran, Sensors Actuators B 226 (2016) 318–325.
[54] Q. Zhang, Y. Jiang, Y. Zhang, Z. Ye, W. Tan, M. Lang, Polym. Degrad. Stab. 98 (2013) 209–218.
[55] M. Bognitzki, W. Czado, T. Frese, A. Schaper, M. Hellwig, M. Steinhart, A. Greiner, H.J. Wendorff, Adv. Mater. 13 (2001) 70–72.
[56] S. Megelski, J.S. Stephens, D.B. Chase, J.F. Rabolt, Macromolecules 35 (2002) 8456–8466.
[57] R.A. Pérez, J.-E. Won, J.C. Knowles, H.-W. Kim, Adv. Drug Deliv. Rev. 65 (2013) 471–496.